BIOLOGICAL SCIENCES: Microbiology

Mechanism for nitrogen isotope fractionation during ammonium assimilation by

Escherichia coli **K12**

Jason Vo[a,1,2,3,4], William Inwood[a,1,3], John M. Hayes[b,1,3,4,5], Sydney Kustu[a,1,3,4,5]

[a]Department of Plant and Microbial Biology, University of California at Berkeley, Berkeley, CA 94720

[b]Woods Hole Oceanographic Institution, Woods Hole, MA 02543

John Hayes

1862 Tacoma Ave.

Berkeley, CA 94707

Phone: 510-479-5220

Email: jhayes@whoi.edu

[1]Designed research

[2]Performed research

[3]Analyzed data

[4]Wrote the paper

[5]Contributed equally to this work

Abstract

Organisms that use ammonium as the sole nitrogen source discriminate between [^{15}N] and [^{14}N]ammonium. This leaves an isotopic signature in their biomass that depends on the external concentration of ammonium. To dissect how differences in discrimination arise molecularly we examined a wild-type strain of *E. coli* K12 and mutant strains with lesions affecting ammonium-assimilatory proteins. We used isotope-ratio mass spectrometry to assess the nitrogen isotopic composition of cell material when the strains were grown in batch culture at either high or low external concentrations of NH_3 (achieved by controlling total NH_4Cl and pH of the medium). At high NH_3 (≥ 0.89 μM), discrimination against the heavy isotope by the wild-type strain (-19.2‰) can be accounted for by the equilibrium isotope effect for dissociation of NH_4^+ to $NH_3 + H^+$. NH_3 equilibrates across the cytoplasmic membrane and glutamine synthetase does not manifest an isotope effect *in vivo.* At low NH_3 (≤ 0.18 μM), discrimination reflects an isotope effect for the NH_4^+ channel AmtB (-14.1‰). By making *E. coli* dependent on the low-affinity ammonium-assimilatory pathway, we determined that biosynthetic glutamate dehydrogenase has an inverse isotope effect *in vivo* (+8.8‰). Likewise, by making unmediated diffusion of NH_3 across the cytoplasmic membrane rate-limiting for cell growth in a mutant strain lacking AmtB, we could deduce an *in vivo* isotope effect for transport of NH_3 across the membrane (-10.9‰). The paper presents the raw data from which our conclusions were drawn and discusses the assumptions underlying them.

53 **/body**

54 **Introduction**

55 Fractionation of heavy and light isotopes of nitrogen (^{15}N vs. ^{14}N), carbon (^{13}C vs. ^{12}C) and

56 hydrogen (D vs. H) can provide information about metabolic pathways and reaction mechanisms

57 within living organisms (1–4). For example, fractionation between ^{15}N and ^{14}N during

58 incorporation of ammonium N in a single-celled organism like *E. coli* is determined by the rate-

59 limiting step for assimilating it into glutamate, the precursor of 88% of cellular nitrogen-

60 containing material (5). All nitrogen assimilated into this central metabolic intermediate goes on

61 to be incorporated into cell material. Transfers from glutamate to other molecules are direct.

62 Although transfers from glutamine, including that to glutamate, involve deamidation, the NH_3

63 released is carried directly to the assimilatory catalytic site through a tunnel and hence cannot be

64 protonated or diffuse away (6). The overall ratio of ^{15}N to ^{14}N in biomass is thus controlled by a

65 step(s) at or prior to assimilation of ammonium N into glutamate.

66

67 In *E. coli*, the proteins participating in early and potentially rate-determining steps in the

68 incorporation of NH_4^+ into glutamate are: 1) AmtB, its only membrane channel for NH_4^+(7); 2)

69 glutamine synthetase (GS), the first enzyme of the high-affinity ammonium-assimilatory pathway;

70 3) glutamate synthase [glutamine(amide) 2-oxoglutarate amino transferase], GOGAT; and 4)

71 glutamate dehydrogenase (GDH), the first enzyme of the low-affinity ammonium-assimilatory

72 pathway (Fig. 1; reviewed in (8)). To study effects of these proteins on the *in vivo* fractionation of

73 ammonium N we used wild-type and genetic mutant strains in which one or more was lacking or

74 defective and studied these strains at high or low external concentrations of NH_3. To decrease the

75 concentration of external NH_3 and still achieve significant cell yield, we lowered both the total

76 concentration of NH_4Cl and the pH of the medium. Though *E. coli* lives in the human gut, which is

77 nitrogen-rich, it also survives in fresh and brackish water, in which supplies of available

78 ammonium can be limited (9, 10). Moreover, it acidifies its own environment by fermentation.

3

79 Accordingly, the conditions we have chosen to study the behavior of *E. coli* at low external NH_3 are

80 pertinent to its normal life cycle.

81

82 Ammonium ($NH_4^+ + NH_3$) is the optimal nitrogen source for *E. coli*, *i. e.*, that which yields most

83 rapid growth. Ammonium [pKa = 9.25] enters cells in two forms (Fig. 1). NH_3, which is ~ 2% of

84 total ammonium at pH 7.4, crosses the cell membrane by unmediated diffusion, a process that

85 cannot be altered genetically. When the pH is decreased to 5.5, NH_3 is only ~ 0.02% of total

86 ammonium. NH_4^+, which is the bulk of total ammonium at both pH 7.4 and pH 5.5, can enter the

87 cells if and only if the AmtB channel is expressed and functional. Its expression is controlled at the

88 transcriptional level and is regulated largely by the free-pool concentration of glutamine in the cell

89 interior (8), whereas its activity is controlled by the regulatory protein GlnK, largely in response to

90 the free-pool concentration of the precursor metabolite 2-oxoglutarate, which is an intermediate

91 in the tricarboxylic acid cycle ((11) and references cited therein). Expression of AmtB increases as

92 the glutamine concentration declines and the channel is activated as the concentration of 2-

93 oxoglutarate rises.

94

95 Within the cell, N is assimilated into glutamate, the organic precursor of most cellular nitrogen, by

96 a high-affinity cycle and by a low-affinity enzyme (Fig. 1). The high-affinity cycle is constituted by

97 the exquisitely regulated GS and by GOGAT. The low-affinity enzyme is biosynthetic (NADPH-

98 dependent) GDH (8). Use of one mol of ATP per glutamate synthesized in the GS/GOGAT cycle

99 drives assimilation of N even at extremely low concentrations of ammonium but is apparently

100 detrimental when ammonium is abundant and energy is limiting (12). Both GS and GDH use NH_3

101 as their substrate because bond formation requires the lone pair of electrons on the N of NH_3 (6,

102 13). Hence, NH_4^+ must be dissociated to $NH_3 + H^+$ before either enzyme can use it. An equilibrium

103 isotope effect associated with this spontaneous process leads to depletion of ^{15}N in NH_3 relative to

4

104   NH_4^+. Its magnitude is -19.2‰ (weighted mean, std. error = 0.4‰, n = 3; (14)). That is, at

105   equilibrium, $^{15}N/^{14}N$ in NH_3 is 19.2 parts per thousand lower than that in NH_4^+.

106

107   To control the site of rate limitation, we employed well-characterized mutant strains (Table 1).

108   One such strain ($\Delta amtB$) lacked AmtB. A second strain (AmtBΔC-term) had a poorly active AmtB

109   channel in which the normal membrane pores lacked the usual carboxy-terminal cytoplasmic

110   extensions (15, 16). A third strain ($\Delta gdhA$::kan) lacked GDH, the low-affinity ammonium-

111   assimilatory enzyme. The last two strains ($gltD$::kan and $gltD$::kan$\Delta amtB$) lacked GOGAT (Table 1;

112   (8)). We did not employ a mutant lacking GS because this strain is auxotrophic for glutamine and

113   requires that glutamine be added to the medium in high concentrations even in the presence of

114   high concentrations of ammonium (17). We studied the mutant strains and their parental strain,

115   which is a physiologically robust *E. coli* K12 wild-type (18, 19), under both ammonium-excess and

116   limiting conditions. We determined doubling time, cell yield, residual ammonium in the medium,

117   and the isotopic fractionation associated with incorporation of ammonium into cell material (see

118   Materials and Methods). When the absence or alteration of one protein increased the doubling

119   time of the strain (*i. e.*, decreased the growth rate), we could determine the rate-limiting step in

120   transport or assimilation.

121

122   **Results**

123   *Parental wild-type strain*. The doubling time was 50 min. at all values of c_0, the initial external

124   concentration of ammonia (*n. b.*, NH_3, not NH_3 + NH_4^+; Table 2, Fig. 2A). For $0.89 \leq c_0 \leq 280$ μM,

125   measured isotopic fractionations (ε_b) ranged from -16.1 to -23.8‰ (mean and std. dev. -19.2 ±

126   2.6‰ n = 7), with negative values of ε indicating depletion of ^{15}N in the biomass relative to the

127   dissolved inorganic N in the medium (Table 2). At lower concentrations ($c_0 \leq 200$ nM), *i. e.*, at 1.0

128   or 0.5 mM total ammonium and pH = 5.5, the isotopic fractionation decreased to -8.1 or -5.4‰,

129   respectively (Table 2, Fig. 2B). AmtB is highly expressed even when the concentration of external

130   NH_3 is 5 to 10 times higher, namely 1 μM (5 mM total ammonium at pH 5.5; (11)), but its activity is

131   not needed for optimal growth and it is inhibited by the regulatory protein GlnK (20–22). AmtB is

132   not expressed when external NH_3 is 10 μM (0.5 mM total ammonium at pH 7.4) or higher (11, 23).

133

134   *GDH⁻ strain*. The GDH⁻ strain ($\Delta gdhA$::kan) lacks the low-affinity pathway for ammonium

135   assimilation and hence is completely dependent on the high-affinity pathway for synthesis of

136   glutamate and glutamine. Its doubling time was indistinguishable from that of wild type under all

137   conditions of nitrogen availability and its isotopic fractionations were very similar to those of the

138   wild-type strain (Table 2). For $0.89 \leq c_0 \leq 280$ μM, ε_b ranged from -18.8 to -25.4‰ (mean and std.

139   dev. -21.3 ± 2.6‰, $n = 7$). For $c_0 = 89$ nM, ε_b decreased to -6.1‰. Because the ranges of ε_b for cells

140   having or lacking GDH overlap, these observations strongly support earlier reports that the GS-

141   GOGAT cycle is the primary means for incorporating ammonium into biomass at all concentrations

142   of NH_3 (12, 24, 25).

143

144   *GOGAT⁻ strains*. The GOGAT⁻ strain (*gltD*::kan) lacks the high-affinity ammonium-assimilatory cycle

145   and depends on the linear, low-affinity pathway (biosynthetic, NADPH-dependent GDH) for

146   synthesis of glutamate. GS converts approximately 12% of the glutamate product of GDH to

147   glutamine to meet biosynthetic needs. When initial external concentrations of NH_3 were decreased

148   from 70 to 7 μM, the doubling time of the strain increased from 50 to 65 min. (Table 2, Fig. S1A)

149   and hence the activity of GDH [*E. coli.* has only a biosynthetic GDH (26)] was apparently rate-

150   limiting for cell growth under these conditions. The weighted-mean isotopic fractionation

151   was -11.2‰ (std. error = 0.3‰, $n = 3$) at both concentrations of NH_3 (Fig. S1D). This strain did not

152   grow at all at $c_0 \leq 1$ μM (23).

153

154   In agreement with its dependence on the low-affinity enzyme, GDH, for synthesis of glutamate,

155   *gltD*::kan has an abnormally low internal-free-pool concentration of glutamate at low NH_3 (27).

156   The *gltD*::kan strain also has an unusually high free-pool concentration of glutamine (27–29), the

157   primary metabolic indicator of nitrogen sufficiency and hence the primary metabolic regulator of

158   the transcriptional response to nitrogen availability (8, 27). This strain fails to express a number

159   of proteins under the control of nitrogen regulatory protein C (NtrC), which is active at low

160   internal concentrations of glutamine (8, 30).

161

162   Although we presumed that AmtB, which is one of the proteins controlled by NtrC, was poorly

163   expressed (23, 31), we constructed a double-mutant strain (*gltD*::kan$\Delta amtB$) to be certain that

164   AmtB was completely absent. The doubling time of the *gltD*::kan$\Delta amtB$ strain was slightly longer

165   than that of the *gltD*::kan strain but the isotopic fractionation was unchanged at -10.3‰ (Table 2,

166   Fig. S1D).

167

168   *AmtB-and AmtB-defective strains*. Finally, the AmtB$^-$ strain ($\Delta amtB$) lacks the NH_4^+ channel. For

169   acquisition of ammonium it must depend on unmediated diffusion of NH_3 across the cytoplasmic

170   membrane. At high external concentrations of NH_3, both the doubling time of the $\Delta amtB$ strain and

171   its isotopic fractionation were identical to those of the wild-type and of the $\Delta gdhA$ strain (Table 2).

172   In fact, under these conditions, the wild type does not transcribe the *glnKamtB* operon (11, 23,

173   31). When the external concentration of NH_3 was decreased to 1 μM, the $\Delta amtB$ strain grew very

174   slowly; its doubling time was initially 200 min. and growth slowed even more as the strain

175   consumed ammonium and thereby decreased the external NH_3 concentration further (11, 23).

176   Under these conditions, the weighted-mean isotopic fractionation was -30.1‰ (std. error = 0.6‰,

177   *n* = 2), markedly larger than that observed in other strains.

178

179   For the strain in which the AmtB protein was modified at the carboxyl terminal (AmtBΔC-term;

180   (15, 16)), both the doubling time and isotopic fractionation at c_0 = 0.89 μM did not differ from

181   those of the wild-type, GDH$^-$, and AmtB$^-$ strains (Table 2). However, when c_0 was decreased to 89

7

182 nM, AmtBΔC-term had a doubling time of 110 min., more than twice as long as that of the wild

183 type and approximately half as long as that of Δ*amtB*. Under this condition, the activity of AmtB

184 appeared to be rate-limiting for growth and the weighted-mean ε_b was -17.6‰ (std. error

185 = 0.3‰, *n* = 2).

186

187 *Process-related summary of isotopic observations.* Table 2 includes 11 different observations of ε_b

188 for cells equilibrating NH_3 by diffusion and having both the low- and high-affinity pathways for its

189 assimilation (Fig. 1). These include seven wild-type cultures with $0.89 \leq c_0 \leq 280$ μM, three Δ*amtB*

190 cultures with $0.89 \leq c_0 \leq 70$ μM and one AmtBΔC-term strain with $c_0 = 0.89$ μM. Values of ε_b range

191 from -16.1 to -23.8‰. The weighted mean is -19.6‰ (std. error = 0.7‰). There were seven

192 different observations for cells equilibrating NH_3 by diffusion and lacking the low-affinity GDH

193 pathway for its assimilation. For these Δ*gdhA* cultures, as for wild-type, $0.89 \leq c_0 \leq 280$ μM. Values

194 of ε_b range from -18.8 to -25.4‰. The weighted mean is -22.2‰ (std. error = 0.9‰). In total,

195 there are 18 different observations of ε_b for cells equilibrating NH_3 by diffusion and using the high-

196 affinity GS-GOGAT cycle to incorporate ammonium N into organic molecules. Values of ε_b range

197 from -16.1 to -25.4‰. The weighted mean is -21.1‰ (std. error = 0.6). Variations of ε_b are not

198 correlated with c_0 (r^2 = 0.13). Three values of ε_b were obtained for cells relying on the AmtB

199 channel for transport of NH_4^+ and assimilating ammonium N *via* GS + GOGAT. In those cases, two

200 wild-type cultures with $c_0 = 0.089$ and 0.18 μM and one Δ*gdhA* culture with $c_0 = 0.089$ μM, ε_b

201 ranged from -5.4 to -8.1‰. In four cases, cells incorporated N using GS + GOGAT but either had no

202 AmtB channel or an AmtB channel that was impaired by deletion of the C-terminal extensions.

203 When AmtB was entirely absent (two cases, $c_0 = 0.18$ and 0.089 μM), weighted-mean ε_b was

204 -30.1‰. When AmtB was only modified ($c_0 = 0.089$ μM, two cases), the weighted-mean ε_b was

205 -17.6‰. Finally, when cells lacked GOGAT (three cultures of Δ*gltD* and one of Δ*gltDamtB*::kan),

206 values of ε_b varied from -10.3 to -11.5‰ with a weighted mean of -10.5‰ (std. error = 0.2‰).

207

8

Discussion

When external concentrations of NH_3 exceed 0.18 μM, NH_3 can rapidly equilibrate across the cytoplasmic membrane of many bacteria by unmediated diffusion and NH_4^+ channels are not expressed (7, 11, 23, 32–34). The interior pool of NH_3 (in equilibrium with intracellular NH_4^+) has only one input, diffusion of NH_3 from the external medium. Though it has three potential outputs—assimilation of NH_3 by GS, assimilation of NH_3 by GDH, and leakage from the cell—our results are not significantly affected by the absence of GDH (see Process-related summary), which reduces the outputs to two. The isotopic budget is summarized in Fig. 3A. Balancing the input against the outputs, we can write

[1] $\delta_{ae} + \varepsilon_{at} = g(\delta_{ai} + \varepsilon_{GS}) + (1 - g)(\delta_{ai} + \varepsilon_{at})$

where the δ values are defined in Fig. 3A, ε_{at} is the isotope effect associated with transport of NH_3 across the membrane, and g is the fraction of the input that is incorporated into biomass. When equilibration of NH_3 across the membrane is rapid in comparison to the rate of assimilation, $g \rightarrow 0$ (*n. b.*, g is not the *amount* of NH_3 that is assimilated but instead the *fraction* which is assimilated) and $\delta_{ae} = \delta_{ai}$. Because $\delta_b = \delta_{ai} + \varepsilon_{GS}$, the isotopic composition of the external NH_3 is related to that of the cells by $\delta_{ae} = \delta_b - \varepsilon_{GS}$. Since essentially all external N is in the form of NH_4^+, $\delta_{ae} = \delta_e + \varepsilon_h$, where δ_e is the measured isotopic composition of the N supplied to the medium and ε_h is the equilibrium isotope effect relating NH_4^+ and NH_3. Finally, recalling that measured values of ε_b are equal to $\delta_b - \delta_e$, we obtain $\varepsilon_{GS} = \varepsilon_b - \varepsilon_h$. As noted above and summarized in Table 3, 18 experiments yielded $\varepsilon_b \sim -21.1‰$. The 95% confidence interval of that value overlaps with the 95% confidence interval for ε_h. Accordingly, there is no evidence for fractionation by GS.

An alternative interpretation, with g appreciably greater than zero, is not tenable. Specifically, the 18 experiments yielding $\varepsilon_b \approx \varepsilon_h$ could then be explained only if (*i*) g, ε_{GS}, and ε_{at} happened in all

9

234   cases to have values satisfying the relationship $g = \varepsilon_{GS}/(\varepsilon_{GS} - \varepsilon_{at})$ and (*ii*) g was independent of the

235   external concentration of NH_3. Additionally, a well documented experimental study of nitrogen

236   and carbon isotope effects associated with glutamine synthetase from *E. coli* found a near-zero

237   nitrogen isotope effect of -0.7 ± 0.6‰ (mean and standard deviation, *n* = 7, (35)).

238

239   It is unlikely that GS limits growth because it is synthesized in excess when supplies of NH_3 are

240   plentiful and its catalytic activity is regulated downwards by covalent modification (36–38). It is

241   more likely that the flux of N into glutamate, the most plentiful intermediate in central nitrogen

242   metabolism, is limited by the capacity of GOGAT. No isotopic fractionation is associated with

243   GOGAT because practically all of the amide N in gln is transferred to 2-oxoglutarate to produce glu.

244

245   When external NH_3 concentrations are below 0.89 µM, *E. coli* K12 depends on the ammonium

246   channel AmtB to maintain an optimal growth rate. Cells lacking this channel ($\Delta amtB$) depend on

247   uncatalyzed transport of NH_3 across the membrane. At $c_0 \leq 0.2$ µM, growth of the $\Delta amtB$ strain is

248   extremely slow and the rate decreases as the external concentration of NH_3 declines (Table 2, Fig.

249   2A). The mass balance described by Eq. 1 applies but the conditions differ from those just

250   discussed. Instead, $g \neq 0$ and, because GS imposed no fractionation even when supplies of NH_3

251   were abundant, we know that $\delta_{ai} = \delta_b$ and $\varepsilon_{GS} = 0$. Making these substitutions and simplifying, we

252   obtain $\delta_{ae} = \delta_b - g\varepsilon_{at}$. Substituting $\delta_{ae} = \delta_e + \varepsilon_h$ and $\varepsilon_b = \delta_b - \delta_e$ leads to $\varepsilon_b = g\varepsilon_{at} + \varepsilon_h$. At the limit in

253   which growth is limited by transport of NH_3 and $g \rightarrow 1$, $\varepsilon_{at} = \varepsilon_b - \varepsilon_h$. If the slowest growing cultures

254   (experiments 27 and 1, Table 2) represent that case, $\varepsilon_{at} = -30.1 + 19.2 = -10.9 \pm 0.7$‰ (std. error

255   from combining 0.5 and 0.4 in quadrature). This relatively large value suggests that transport of

256   NH_3 across the membrane is limited by some process other than simple diffusion. Polar

257   interactions within the membrane may play a role. Rishavy and Cleland (39) commented that the

258   isotope effect in a related case "could easily be 2%" (*i. e.*, 20‰, almost twice that estimated here).

259

260   For cells with a normal AmtB channel (wild-type or $\Delta gdhA$ strain) and with $c_0 = 0.089$ μM, ε_b was

261   observed as low as -5.4 ± 0.3‰, much lower than that of a strain lacking the channel ($\Delta amtB$). The

262   corresponding mass balance is shown schematically in Fig. 3B and expressed mathematically in

263   Eq. 2.

264

265   [2] $\delta_e + \varepsilon_{ht} = g\delta_b + (1 - g)(\delta_b + \varepsilon_{at})$

266

267   Here, ε_{ht} is the isotope effect associated with transport of NH_4^+ by the AmtB channel and

268   substitutions introduced above have been adopted where appropriate ($\delta_{he} = \delta_e$, $\delta_{ai} = \delta_b$).

269   Simplifying gives $\varepsilon_b = \varepsilon_{ht} - (1 - g)\varepsilon_{at}$. A recent quantitative study of AmtB function (11) indicates

270   that g is ~ 0.2. For $\varepsilon_b = -5.4‰$, adopting $\varepsilon_{at} \approx -10.9‰$ (see above), we find $\varepsilon_{ht} = -14.1‰$. If an

271   uncertainty of 0.05 is assigned to g, the estimated std. error of ε_{ht} is 0.7‰. Notably, the reduced

272   fractionation at low values of c_0, a condition that may be encountered in nature, derives not only

273   from fractionations associated with the AmtB channel but from an interplay between

274   fractionations associated with ε_{ht} and ε_{at}.

275

276   When the wild-type strain was grown with a slightly higher $c_0 = 0.18$ μM, the observed

277   fractionation increased to -8.1‰. The AmtB channel also functions at this NH_3 concentration

278   because an AmtB⁻ strain continues to grow suboptimally. Hence eq'n 2 applies. Using $\varepsilon_{ht} = -14.1 \pm$

279   0.7‰ and solving for g, we find $g = 0.45 \pm 0.1$. When AmtB functions, the internal ammonium

280   concentration is held constant and hence there is less leakage of NH_3 at higher external NH_3

281   concentrations (11).

282

283   For cells with an altered AmtB channel lacking the cytoplasmic C-terminal extensions (16), $\varepsilon_b =$

284   -17.6 ± 0.3‰ (wt'd. mean and std. error) at $c_o = 0.089$ uM. The fraction of N assimilated by GS is

285   0.5 (11) and solving as above yields $\bar{\varepsilon}_{ht}' = -23.0 \pm 0.7‰$ (where a prime is used to denote the

11

286   altered channel). If the uncertainty assigned to g is doubled (to 0.1), the standard error increases

287   only to ± 1.2‰. Hence the isotope effect for the mutant AmtB channel is significantly larger than

288   that for the wild-type channel. The mutant channel is known to lack coordination between the

289   function of its individual monomers and to have other unusual properties (40).

290

291   To make *E. coli* dependent on the low-affinity pathway for assimilation of ammonium we

292   inactivated GOGAT. This eliminates the GOGAT cycle and makes the organism dependent on

293   biosynthetic GDH. At an external NH_3 concentration of 10 µM, GDH activity already limits the

294   growth rate of the GOGAT$^-$ strain, and the strain does not grow at all at $c_0 = 1$ µM. The fractionation

295   observed for the GOGAT$^-$ strains with $c_0 \geq 7$ µM is -10.5‰. Assuming that NH_3 inside and outside

296   the cell was in equilibrium, as for the wild-type, $\Delta gdhA$, and $\Delta amtB$ strains at the same

297   concentrations, it follows that internal NH_3 was depleted in ^{15}N by 19.2‰ relative to external

298   dissolved inorganic N and, therefore, that the observation of ε_b = -10.5‰ requires inverse

299   fractionation of ^{15}N by GDH (*i. e.*, enrichment of the product relative to the reactant) with

300   ε_{GDH} = 8.7 ± 0.4‰. An inverse isotope effect has also been reported for bovine liver GDH (41).

301

302   *Conclusion.* Our studies of *E. coli* K12 have yielded *in vivo* isotope effects as summarized in Table 3.

303   To our knowledge, the isotope effect for transport of NH_3 is the first for a biological membrane. A

304   previous measurement was made *in vitro* with a membrane filter (14).

305

306   That ε_b for the $\Delta gdhA$ strain is the same as that for the wild-type strain at all external

307   concentrations of NH_3 confirms the finding of Yuan et al. (24, 25) that the GOGAT cycle is the

308   major means for assimilation of NH_3 by *E. coli* K12 not only at low but also at high concentrations.

309   Although the GOGAT cycle is widespread in bacteria and archaea (8, 42, 43), whereas the

310   occurrence of biosynthetic GDH appears to be more restricted (44), several important examples of

311   organisms naturally lacking GOGAT have recently come to light (45). Determining ε_b for the

312   abundant ocean archaean *Nitrosopumilis maritima* will be particularly interesting not only

313   because it lacks GOGAT and depends on GDH for ammonium assimilation but also because it

314   oxidizes ammonium extracellularly as its primary energy source.

315

316   We hope that the present results will help future workers to correlate environmental genomic

317   data with isotopic variations observed in nature.

318

319   *Comparison to earlier work.* Studying the γ-proteobacterium *Vibrio harveyi*, a close evolutionary

320   relative of *E. coli* K12, Hoch *et al*. (46) also found that isotopic fractionation between external

321   ammonium and cell material varied with external ammonium availability. Now, by using AmtB$^-$

322   strains, we have determined that the decrease in ε_b from ~ -20‰ to -4‰ that they observed as

323   external ammonium was dropped from an initial concentration of ~500 to ~25 μM (pH 7.4) did, as

324   they proposed, depend on the activity of an active ammonium channel. Specifically, ε_b ~ -5‰

325   results from (*i*) acquisition of NH_4^+ rather than NH_3 by the growing cells, (*ii*) an isotope effect

326   associated with transport of NH_4^+ by the AmtB channel (ε_{ht} ~ -14‰), (*iii*) equilibration of NH_4^+

327   and NH_3 inside the cell, (*iv*) an absence of isotopic fractionation during assimilation of NH_3 by GS,

328   and (*v*) leakage of ^{15}N-depleted NH_3 from the cells.

329

330   Given the very large ε_b characteristic of *E. coli* AmtB$^-$ strains at low external NH_3 (-30‰), which

331   appears to result from rate-limiting diffusion of NH_3 across the cytoplasmic membrane, it is

332   tempting to speculate that the fractionation observed in *V. harveyi* as the external concentration of

333   ammonium decreased from 182 to 107 μM in a single experiment [ε_b = -26.5‰; (46)] may

334   indicate the precise range of external ammonium concentrations at which unmediated diffusion of

335   NH_3 becomes limiting in wild-type *V. harveyi*, just prior to activation of its AmtB channel. In *E. coli*

336   expression of AmtB occurs in response to a decrease in the internal-free-pool concentration of

337   glutamine, whereas activation requires, in addition, an increase in the pool concentration of its

13

338   precursor metabolite 2-oxoglutarate (11). The latter occurs at lower external NH_3 concentrations

339   than the former. Activation requires release of the inhibitory gating protein GlnK (20–22).

340

341   Finally, we think that the decrease in ε_b from -21 to -14‰, which Hoch *et al.* observed above 5 mM

342   external ammonium, is an artifact of growth inhibition (doubling time increased from the optimal

343   of 84 min. to 138 min. at high ammonium). Whatever the explanation, the ε_b of -14‰ cannot be

344   characteristic of GDH, as they proposed, because the NADH-dependent GDH they characterized is

345   a catabolic enzyme. The genome sequence of *V. harveyi* is now known and it apparently lacks a

346   biosynthetic, NADPH-dependent GDH. Moreover, we find that the biosynthetic, NADPH-dependent

347   GDH of *E. coli* contributes very little to ammonium assimilation even at 20 mM ammonium, their

348   highest concentration and ours.

349

350   **Materials and Methods**

351   **Bacterial Strains and Cultures.** NCM3722 (18) was the parental strain for all genetic mutant

352   strains used in this work (Table 1). Additional details of strain construction are in SI Materials and

353   Methods. For growth experiments, bacterial cultures were grown on the minimal medium of

354   Neidhardt et al. (47) in MOPS buffered medium, pH 7.4, with 0.1% glucose as sole carbon source

355   and NH_4Cl as sole nitrogen source. For experiments at pH 5.5, cultures were additionally adapted

356   to low pH in minimal medium buffered with MES at pH 5.5.Growth and doubling time were

357   determined by measuring optical density at 420 nm.

358

359   **Ammonia Assay.** Residual ammonium in cell-free supernatants was assayed in a GDH catalyzed

360   reaction (AA0100 kit, Sigma). In the assay 2-oxoglutarate is reduced to L-glutamate by GDH using

361   ammonium as substrate and NADPH as the cofactor providing reducing equivalents. Oxidation of

362   NADPH is measured by a change in absorbance at 340 nm.

363

14

Sample Preparation and Isotopic Analyses. Bacterial cell samples were taken at various points during growth and were removed from the supernatant by high-speed centrifugation. The cell-free supernatant was frozen at -80°C for later measurement of residual ammonium, glucose, and final pH. The cells were washed twice in medium without additional glucose or ammonium, and dried in air overnight. Uniform amounts of 2 mg dry weight yielding 0.8 mg carbon and 0.2 mg nitrogen were transferred into pre-weighed tin capsules (part number 240-053-00, Costech Analytical Technologies, Inc.). Capsules containing only the reactant glucose and ammonium chloride used in the media were also prepared. All samples were analyzed at the UC Berkeley Center for Stable Isotope Biogeochemistry. $\delta^{15}N$ and %N were determined by using a PDZ Europa system consisting of an ANCA-NT carbon/nitrogen analyzer in combination with a 2020 mass spectrometer (48). The isotopic-abundance parameters are defined as follows:

[3] $\delta^{15}N = 10^3[(^{15}R_{sample}/^{15}R_{standard}) - 1]$

Where $^{15}R \equiv {}^{15}N/^{14}N$ and the isotopic standard for nitrogen is N_2 in air, for which $^{15}R = 0.0036765$ (49). Values of $\delta^{15}N$ express the relative difference between the isotope ratio in the sample and in the standard, expressed in parts per thousand (‰). A value of $\delta^{15}N = -12.2$‰, for example, indicates that $^{15}R_{sample}$ is 0.0036316. The precision of the analyses, expressed as a standard deviation of a single observation and based on five pairs of duplicates and four sets of triplicates collected during the analyses (thus 13 degrees of freedom) is 0.06‰.

Calculations. The objective of the isotopic analyses is to determine ε_b, the overall isotope effect associated with the assimilation of N. This is most simply expressed by the isotopic difference between the starting pool of inorganic N in the medium and the first increment of biomass formed following inoculation. In mathematical terms, the isotopic difference is expressed as a ratio of isotope ratios. Since the isotope ratios are very similar, a notation is used that expresses the

15

390   difference in terms of parts per thousand:

391

392   [4] $\varepsilon_b \equiv 10^3[(^{15}R_{e0}/^{15}R_{b0}) - 1]$

393

394   where $^{15}R_{e0}$ is the ratio of ^{15}N to ^{14}N in the initial medium and $^{15}R_{b0}$ is the same ratio in the first

395   increment of biomass. As growth proceeds, the measured isotopic compositions of both the

396   medium and the biomass change as a result of preferential transfer of either ^{15}N or ^{14}N (depending

397   on the sign of the isotope effect) from the medium to the biomass. Measurements of ε_b must take

398   this into account.

399

400   Here, we employ the regression of δ_b on $[f/(1 - f)]\cdot\ln f$ (1), thus fitting the observations to a linear

401   equation of the form:

402

403   [5] $\delta_b = \delta_0 - [f/(1 - f)]\varepsilon_b\cdot\ln f$

404

405   where δ_b is the measured $\delta^{15}N$ of the biomass, δ_0 is the measured $\delta^{15}N$ of the medium at $t = 0$, and f

406   is the fraction of ammonium unutilized. If, for example, ε_b = -18.8‰, it indicates that ^{15}N is

407   assimilated and used to produce biomass 18.8 parts per thousand more slowly than ^{14}N.

408

409   Values of δ_0 vary between experiments, depending on the batch of NH_4Cl that was used. Specific

410   values are, for experiments 1-5, 3.25 ± 0.19‰ (mean and standard deviation, n = 8); 6-15,

411   1.43 ± 0.06‰ (n = 3); 16-17, 1.12 ± 0.19‰ (n = 2); 18-19, 0.96 ± 0.19‰ (n = 2); 20-21,

412   1.15 ± 0.21‰ (n = 2); 22-24, 1.36 ± 0.09‰ (n = 3); and 25-29, 0.91 ± 0.08‰ (n = 5).

413

414   Uncertainties in ε_b, calculated from the variance about the regression and expressed as standard

415   errors of the slope, are reported in Table 2 and range from 0.1 to 2.9‰. Where weighted means

16

416 are reported, the weighting factor is the inverse variance. The reported standard errors of

417 weighted means are conventional or dispersion-corrected, whichever is greater. Uncertainties

418 reported for calculated isotope effects are derived by conventional propagation of errors.

419

References

1.   Mariotti A et al. (1981) Experimental determination of nitrogen kinetic isotope fractionation: Some principles; illustration for the denitrification and nitrification processes. *Plant Soil* 62:413–430.

2.   Stanley SM (2010) Relation of Phanerozoic stable isotope excursions to climate, bacterial metabolism, and major extinctions. *Proc Natl Acad Sci USA* 107:19185–9.

3.   Valentine DL (2009) Isotopic remembrance of metabolism past. *Proc Natl Acad Sci USA* 106:12565–6.

4.   Zhang X, Gillespie AL, Sessions AL (2009) Large D/H variations in bacterial lipids reflect central metabolic pathways. *Proc Natl Acad Sci USA* 106:12580–6.

5.   Wohlhueter R, Schutt H, Holzer H (1973) in *The Enzymes of Glutamine Metabolism*, eds Prusiner S, Stadtman ER (Academic Press, New York), pp 45–64.

6.   Raushel FM, Thoden JB, Holden HM (2003) Enzymes with molecular tunnels. *Acc Chem Res* 36:539–48.

7.   Fong RN, Kim K-S, Yoshihara C, Inwood WB, Kustu S (2007) The W148L substitution in the Escherichia coli ammonium channel AmtB increases flux and indicates that the substrate is an ion. *Proc Natl Acad Sci USA* 104:18706–11.

8.   Ikeda TP, Shauger AE, Kustu S (1996) Salmonella typhimurium apparently perceives external nitrogen limitation as internal glutamine limitation. *J Mol Biol* 259:589–607.

9.   Hartl DL, Dykhuizen DE (1984) The population genetics of Escherichia coli. *Annu Rev Genet* 18:31–68.

10.   Van Elsas JD, Semenov A V, Costa R, Trevors JT (2011) Survival of Escherichia coli in the environment: fundamental and public health aspects. *ISME J* 5:173–83.

11.   Kim M et al. (2012) Need-based activation of ammonium uptake in Escherichia coli. *Mol Syst Biol* 8:616.

12.   Helling RB (1994) Why does Escherichia coli have two primary pathways for synthesis of glutamate? *J Bacteriol* 176:4664–4668.

13.   Hartman SC (1973) in *The Enzymes of Glutamine Metabolism*, eds Prusiner S, Stadtman ER (Academic Press, New York), pp 319–330.

14.   Hermes JD, Weiss PM, Cleland WW (1985) Use of nitrogen-15 and deuterium isotope effects to determine the chemical mechanism of phenylalanine ammonia-lyase. *Biochemistry* 24:2959–2967.

15.   Severi E, Javelle A, Merrick M (2007) The conserved carboxy-terminal region of the ammonia channel AmtB plays a critical role in channel function. *Mol Membr Bio* 24:161–71.

16.   Inwood WB, Hall JA, Kim K-S, Fong R, Kustu S (2009) Genetic evidence for an essential oscillation of transmembrane-spanning segment 5 in the Escherichia coli ammonium channel AmtB. *Genetics* 183:1341–55.

17.   Kustu SG, McFarland NC, Hui SP, Esmon B, Ames GF (1979) Nitrogen control of Salmonella typhimurium: co-regulation of synthesis of glutamine synthetase and amino acid transport systems. *J Bacteriol* 138:218–234.

18.   Lyons E, Freeling M, Kustu S, Inwood W (2011) Using genomic sequencing for classical genetics in E. coli K12. *PloS ONE* 6:1–16.

19.   Soupene E et al. (2003) Physiological Studies of Escherichia coli Strain MG1655: Growth Defects and Apparent Cross-Regulation of Gene Expression. *J Bacteriol* 185:5611–5626.

20.   Van Heeswijk WC et al. (1995) An additional PII in Escherichia coli: a new regulatory protein in the glutamine synthetase cascade. *FEMS Microbiol Lett* 132:153–7.

21.   Javelle A, Severi E, Thornton J, Merrick M (2004) Ammonium sensing in Escherichia coli. Role of the ammonium transporter AmtB and AmtB-GlnK complex formation. *The Journal of biological chemistry* 279:8530–8.

22.   Conroy MJ et al. (2007) The crystal structure of the Escherichia coli AmtB-GlnK complex reveals how GlnK regulates the ammonia channel. *Proc Natl Acad Sci USA* 104:1213–8.

23.   Soupene E, He L, Yan D, Kustu S (1998) Ammonia acquisition in enteric bacteria: Physiological role of the ammonium/methylammonium transport B (AmtB) protein. *Proc Natl Acad Sci USA* 95:7030–7034.

24.   Yuan J, Bennett BD, Rabinowitz JD (2008) Kinetic flux profiling for quantitation of cellular metabolic fluxes. *Nat Protoc* 3:1328–40.

25.   Yuan J, Fowler WU, Kimball E, Lu W, Rabinowitz JD (2006) Kinetic flux profiling of nitrogen assimilation in Escherichia coli. *Nat Chem Biol* 2:529–30.

26.   Blattner FR (1997) The Complete Genome Sequence of Escherichia coli K-12. *Science* 277:1453–1462.

27.   Csonka LN, Ikeda TP, Fletcher S a, Kustu S (1994) The accumulation of glutamate is necessary for optimal growth of Salmonella typhimurium in media of high osmolality but not induction of the proU operon. *J Bacteriol* 176:6324–33.

28.   Yan D, Ikeda TP, Shauger AE, Kustu S (1996) Glutamate is required to maintain the steady-state potassium pool in Salmonella typhimurium. *Proc Natl Acad Sci USA* 93:6527–6531.

29.   Yan D (2007) Protection of the glutamate pool concentration in enteric bacteria. *Proc Natl Acad Sci USA* 104:9475–80.

30.   Pahel G, Zelenetz AD, Tyler BM (1978) gltB gene and regulation of nitrogen metabolism by glutamine synthetase in Escherichia coli. *J Bacteriol* 133:139–148.

31.   Van Heeswijk WC et al. (1996) An alternative PII protein in the regulation of glutamine synthetase in Escherichia coli. *Mol Microbiol* 21:133–146.

32.   Boussiba S, Dilling W, Gibson J (1984) Methylammonium transport in Anacystis nidulans R-2. *J Bacteriol* 160:204–210.

33.   Andrade SLA, Einsle O (2007) The Amt/Mep/Rh family of ammonium transport proteins (Review). *Mol Membr Bio* 24:357–365.

34.   Loqué D, Von Wirén N (2004) Regulatory levels for the transport of ammonium in plant roots. *Journal of experimental botany* 55:1293–305.
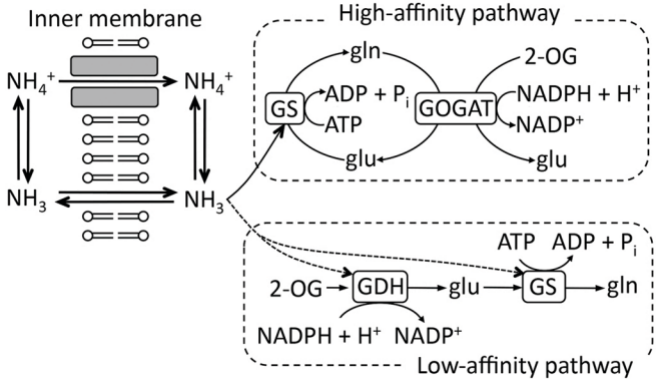
35.   Stoker PW (1994) Heavy-atom isotope effects for enzymes of glutamine metabolism. *PhD thesis (The University of Nebraska - Lincoln)*. Available at: http://digitalcommons.unl.edu/dissertations/AAI9507828 .

36.   Jiang P, Ninfa AJ (2011) A source of ultrasensitivity in the glutamine response of the bicyclic cascade system controlling glutamine synthetase adenylylation state and activity in Escherichia coli. *Biochemistry* 50:10929–40.

37.   Okano H, Hwa T, Lenz P, Yan D (2010) Reversible adenylylation of glutamine synthetase is dynamically counterbalanced during steady-state growth of Escherichia coli. *J Mol Biol* 404:522–36.

38.   Rhee SG, Chock PB, Stadtman ER (1989) Regulation of Escherichia coli glutamine synthetase. *Adv Enzymol Relat Areas Mol Biol* 62:37–92.

39.   Rishavy MA, Cleland WW (1999) 13C, 15N, and 18O equilibrium isotope effects and fractionation factors. *Canadian Journal of Chemistry* 77:967–977.

40.   Inwood WB et al. (2009) Epistatic effects of the protease/chaperone HflB on some damaged forms of the Escherichia coli ammonium channel AmtB. *Genetics* 183:1327–40.

41.   Weiss PM, Chen CY, Cleland WW, Cook PF (1988) Use of primary deuterium and 15N isotope effects to deduce the relative rates of steps in the mechanisms of alanine and glutamate dehydrogenases. *Biochemistry* 27:4814–22.

42.   Dincturk HB, Cunin R, Akce H (2011) Expression and functional analysis of glutamate synthase small subunit-like proteins from archaeon Pyrococcus horikoshii. *Microbiol Res* 166:294–303.

43.   Dincturk HB, Knaff DB (2000) The evolution of glutamate synthase. *Mol Biol Rep* 27:141–148.

44.   Hudson RC, Daniel RM (1993) L-glutamate dehydrogenases: distribution, properties and mechanism. *Comp Biochem Physiol B* 106:767–92.

45.   Walker CB et al. (2010) Nitrosopumilus maritimus genome reveals unique mechanisms for nitrification and autotrophy in globally distributed marine crenarchaea. *Proc Natl Acad Sci USA* 107:8818–23.

46.   Hoch M, Fogel M, Kirchman D (1992) Isotope fractionation associated with ammonium uptake by a marine bacterium. *Limnol Oceanogr* 37:1447–1459.

47.   Neidhardt FC, Bloch PL, Smith DF (1974) Culture Medium for Enterobacteria. *J Bacteriol* 119:736–747.

48.   Brooks PD, Geilmann H, Werner RA, Brand WA (2003) Improved precision of coupled delta13C and delta15N measurements from single samples using an elemental analyzer/isotope ratio mass spectrometer combination with a post-column six-port valve and selective CO2 trapping; improved halide robustness of the co. *Rapid Commun Mass Spectrom* 17:1924–6.

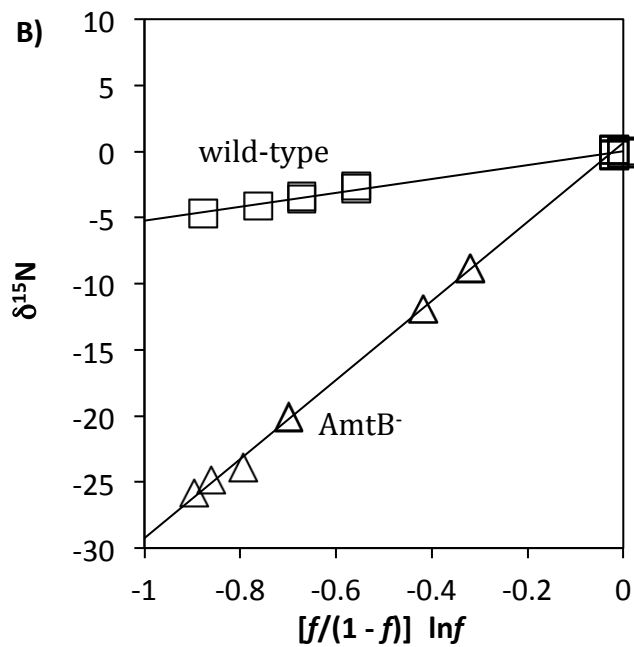49.   Coplen TB, Krouse HR, Bohlke JK (1992) Reporting of nitrogen-isotope abundances. *Pure Appl Chem* 64:907–908.
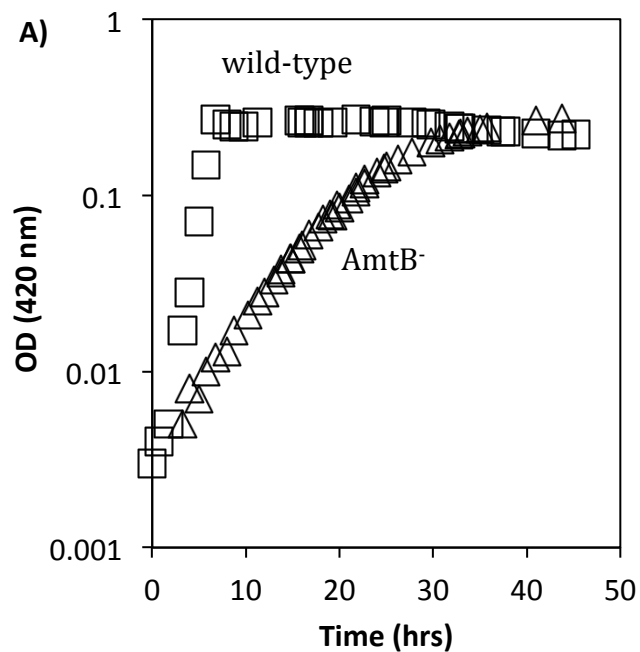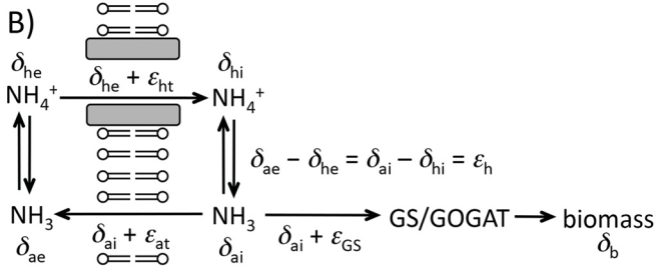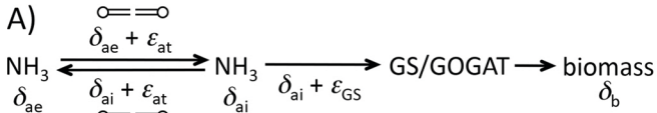
Figure legends

Fig. 1. Schematic diagram of nitrogen assimilation from ammonium by *E. coli* K12.

Fig. 2. Growth (A) and (B) determination of ε_b for assimilation of external ammonium ($c_0 = 0.089$ μM NH_3, 0.5 mM total NH_4Cl, 0.1% glucose, pH 5.5) into biomass in wild-type (squares) and AmtB⁻ strains (triangles). Cultures in panel B were different from those in panel A, which were sampled more frequently.

Fig. 3. Flows of N across the cell membrane and within cells. Isotopic compositions are denoted by δ terms and isotope effects are denoted by ε terms. In subscripts, a designates NH_3; b,biomass; e,external; GS,glutamate synthetase; h,NH_4^+ or protonation; i,internal; and t,transport. Isotopic compositions of the N fluxes are then given by expressions such as $\delta_{he} + \varepsilon_{ht}$, which indicates the isotopic composition of the ammonium being transported by the AmtB channel. (A) Cells not utilizing the AmtB channel to actively transport NH_4^+. (B) Cells in which the AmtB channel is used.

Inner membrane

High-affinity pathway

Low-affinity pathway

A) — OD (420 nm) vs Time (hrs); wild-type (squares) and AmtB⁻ (triangles)

B) — δ¹⁵N vs [f/(1 - f)] lnf; wild-type and AmtB⁻

Table 1. Bacterial strains[*]

Strain: Genotype	Phenotype
NCM3722: *E. coli* K12 wild-type	wild-type
NCM4199: *amtB, tesB::*kan	AmtBΔC-term[†]
NCM4453: *gltD*::kan	GOGAT^{-}[‡]
NCM4454: *ΔgdhA*::kan	GDH^{-}[‡]
NCM4590: *ΔamtB*	AmtB^{-}
NCM4701: *gltD::kanΔamtB*	GOGAT^{-}, AmtB^{-}

[*]All strains were constructed in the background of a physiologically robust *E. coli* K12 wild-type strain, NCM3722 ((18, 19); see Materials and Methods).

[†] Residues from position 382 onward were deleted (15, 16).

[‡] Dalai Yan, Indiana University School of Medicine.

Table 2. Summary of cultures and measured isotopic fractionations

Exp.	Strain[*]	c_0 (NH$_3$)[†] μM	D.T.[‡] min.	n[§]	ε_b[¶] ‰
17	NCM3722	*280*	50	8	-20.4 ± 2.1
23	NCM3722	*280*	50	7	-16.8 ± 1.9
16	NCM3722	*140*	50	8	-16.1 ± 0.7
22	NCM3722	*140*	50	7	-18.2 ± 1.1
8	NCM3722	*70*	50	9	-19.1 ± 1.4
10	NCM3722	*7*	50	5	-23.8 ± 1.4
5	NCM3722	*0.89*	50	6	-20.0 ± 1.0
26	NCM3722	*0.18*	50	6	-8.1 ± 0.3
2	NCM3722	*0.089*	50	5	-5.4 ± 0.3
9	NCM4590	*70*	50	9	-19.9 ± 1.7
11	NCM4590	*7*	50	4	-22.2 ± 2.9
3	NCM4590	*0.89*	50	8	-20.3 ± 0.5
27	NCM4590	*0.18*	>100	5	-30.2 ± 0.7
1	NCM4590	*0.089*	>200	6	-29.9 ± 0.9
18	NCM4454	*280*	50	9	-22.1 ± 0.7
21	NCM4454	*280*	50	8	-19.4 ± 2.2
19	NCM4454	*140*	50	7	-25.4 ± 2.9
20	NCM4454	*140*	50	8	-18.8 ± 0.5
15	NCM4454	*70*	50	7	-19.3 ± 1.4
14	NCM4454	*7*	50	4	-20.4 ± 1.4
6	NCM4454	*0.89*	50	8	-23.9 ± 0.4
7	NCM4454	*0.089*	50	5	-6.1 ± 0.6
13	NCM4453	*70*	50	9	-10.3 ± 1.0
12	NCM4453	*7*	65	5	-11.2 ± 0.4
29	NCM4453	*7*	65	5	-11.5 ± 0.5
28	NCM4701	*7*	75	5	-10.3 ± 0.1
24	NCM4199	*0.89*	50	8	-23.3 ± 1.2
25	NCM4199	*0.089*	110	4	-17.2 ± 0.6
30	NCM4199	*0.089*	110	4	-17.8 ± 0.4

[*]Strain number (for phenotype see Table 1).

[†]Concentrations of NH$_3$ determined from total concentrations of NH$_4$Cl, which were 71-fold higher than that of NH$_3$ at pH 7.4 and 5620-fold higher at pH 5.5. Cultures with $c_0 \le 0.89$ were grown at pH 5.5.

[‡]Doubling time.

[§]Number of points used in the determination of ε_b.

[¶]Reported uncertainty is the standard error of the slope derived from the regression described in the section on calculations.

Table 3. Process-related isotope effects

	Process	Related Experiments	Result[*]
1.	Assimilation of NH_3 by GS For $g \to 0$ $\varepsilon_{GS} = \varepsilon_b - \varepsilon_h$	Wild type, $c_0 \geq 0.89$ μM, $n = 7$ AmtB$^-$, $c_0 \geq 0.89$ μM, $n = 3$ AmtBΔC-term, $c_0 = 0.89$ μM, $n = 1$ GDH$^-$, $c_0 \geq 0.89$ μM, $n = 7$	95% Confidence intervals: $\bar{\varepsilon}_b = -21.1 \pm 1.3$‰ $\bar{\varepsilon}_h = -19.2 \pm 1.7$‰ $\varepsilon_{GS} \sim 0$
2.	Transmembrane transport of NH_3 For $g \to 1$ $\varepsilon_{at} = \varepsilon_b - \varepsilon_h$	AmtB$^-$, $c_0 < 0.2$ μM, $n = 2$	$\bar{\varepsilon}_b = -30.1 \pm 0.5$‰ $\varepsilon_{at} = -10.9 \pm 0.7$‰
3.	Transport of NH_4^+ by AmtB $\varepsilon_{ht} = \varepsilon_b + (1 - g)\varepsilon_{at}$	Wild type, $c_0 = 0.089$ μM, $n = 1$ GDH$^-$, $c_0 = 0.089$ μM, $n = 1$	$\bar{\varepsilon}_b = -5.5 \pm 0.3$‰ for $g = 0.2 \pm 0.05$, $\varepsilon_{ht} = -14.1 \pm 0.8$‰
4.	Transport of NH_4^+ by altered AmtB $\bar{\varepsilon}'_{ht} = \varepsilon_b + (1 - g)\varepsilon_{at}$	AmtBΔC-term, $c_0 = 0.089$ μM, $n = 2$	$\bar{\varepsilon}_b = -17.6 \pm 0.3$‰ for $g = 0.5 \pm 0.1$, $\bar{\varepsilon}'_{ht} = -23.1 \pm 1.2$‰
5.	Assimilation of NH_3 by GDH $\varepsilon_{GDH} = \varepsilon_b - \varepsilon_h$	GOGAT$^-$, AmtB$^-$, $c_0 = 7$ μM, $n = 1$ GOGAT$^-$, $c_0 \geq 7$ μM, $n = 3$	$\bar{\varepsilon}_b = -10.5 \pm 0.2$‰ $\varepsilon_{GDH} = 8.8 \pm 0.4$‰

[*]$\bar{\varepsilon}$ denotes weighted mean. Indicated uncertainties are standard errors except for process 1, where 95%confidence intervals are specified.